

Effects of Phosphate on Uranium(VI) Adsorption to Goethite-Coated Sand

TAO CHENG,[†] MARK O. BARNETT,^{*,†}
ERIC E. RODEN,[‡] AND JINLING ZHUANG[†]

Department of Civil Engineering, 238 Harbert Engineering Center, Auburn University, Auburn, Alabama 36849, and Department of Biological Sciences, A122 Bevell Building, Seventh Avenue, University of Alabama, Tuscaloosa, Alabama 35487-0206

U(VI)–phosphate interactions are important in governing the subsurface mobility of U(VI) in both natural and contaminated environments. We studied U(VI) adsorption on goethite-coated sand (to mimic natural Fe-coated subsurface materials) as a function of pH in systems closed to the atmosphere, in both the presence and the absence of phosphate. Our results indicate that phosphate strongly affects U(VI) adsorption. The effect of phosphate on U(VI) adsorption was dependent on solution pH. At low pH, the adsorption of U(VI) increased in the presence of phosphate, and higher phosphate concentration caused a larger extent of increase in U(VI) adsorption. Phosphate was strongly bound by the goethite surface in the low pH range, and the increased adsorption of U(VI) at low pH was attributed to the formation of ternary surface complexes involving both U(VI) and phosphate. In the high pH range, the adsorption of U(VI) decreased in the presence of phosphate at low total Fe concentration, and higher phosphate concentration caused a larger extent of decrease in U(VI) adsorption. This decrease in U(VI) adsorption was attributed to the formation of soluble uranium–phosphate complexes. A surface complexation model (SCM) was proposed to describe the effect of phosphate on U(VI) adsorption to goethite. This proposed model was based on previous models that predict U(VI) adsorption to iron oxides in the absence of phosphate and previous models developed to predict phosphate adsorption on goethite. A postulated ternary surface complex of the form of ($>FePO_4UO_2$) was included in our model to account for the interactions between U(VI) and phosphate. The model we established can successfully predict U(VI) adsorption in the presence of phosphate under a range of conditions (i.e., pH, total phosphate concentration, and total Fe concentration).

Introduction

Uranium (U) is a hazardous element in the environment. Uranium(VI), the thermodynamically stable oxidation state of U in oxic groundwaters, interacts strongly with mineral surfaces, particularly with Fe minerals. Those interactions mitigate the transport of U(VI) in the subsurface, and the importance of Fe minerals in controlling U(VI) adsorption

and transport has been well-documented (1–5). Goethite, a crystalline iron oxyhydroxide (α -FeOOH), is one of the most widespread iron oxides in the soil and sedimentary environments (6) and has a great impact on the mobility of contaminants and nutrients. Goethite is a strong adsorbent for both anions and cations, and the adsorption of phosphate, carbonate, and U(VI) onto goethite has been studied extensively (7–13).

Phosphate, together with carbonate ions and humic substances, are the most important ligands that influence U(VI) adsorption and transport in the subsurface. The effects of carbonate ions on U(VI) adsorption have been studied extensively (1, 2, 11). Phosphate is a much stronger ligand and has been shown to control the subsurface mobility of U(VI) at sites that are used as natural analogues of nuclear waste repositories (14). In addition, the biological reduction of U(VI) to U(IV) by dissimilatory metal-reducing bacteria is currently recognized as a promising strategy for the in situ remediation of U-contaminated subsurface environments (15–17). Phosphorus is an essential nutrient for biological activity; therefore, it could be a required amendment to promote in situ bioremediation via reduction of U(VI) to U(IV). For these reasons, U–phosphate interactions are important in governing the subsurface mobility of U(VI) in both natural and contaminated environments. The presence of phosphate in a system that contains U(VI) and iron oxides might have several potential effects: (i) competition with U(VI) for surface sites on iron oxides, which will decrease U(VI) adsorption; (ii) competition with surface sites for coordination of U(VI) by forming aqueous U(VI)–phosphate complexes, which will decrease U(VI) adsorption; (iii) formation of ternary surface complexes involving both U(VI) and phosphate, which will enhance the adsorption of both U(VI) and phosphate (18, 19); (iv) precipitation of U(VI)–phosphate solids, which could decrease aqueous U(VI) concentration. An extensive literature has examined the influence of U(VI)–phosphate solids on controlling U(VI) mobility, and it has been reported that formation of various types of U(VI)–phosphate solids can dramatically lower U(VI) solubility, reducing U(VI) mobility in contaminated soil and groundwater (20–22). However, there have been relatively few studies on the effects of phosphate on U(VI) adsorption, such as the formation of ternary surface complexes (18).

The purpose of this investigation was to examine the effects of phosphate on U(VI) adsorption onto Fe-coated subsurface materials. Iron oxide grain coatings, formed by weathering processes, have been shown to be important metal-adsorbing phases in aquifers (23). Previously, Barnett et al. (2) and Logue et al. (24) reported that a model independently developed to describe U(VI) adsorption to pure synthetic ferrihydrite could be successfully applied to predict U(VI) adsorption to heterogeneous, iron oxide containing subsurface media. The use of pure iron oxide in batch adsorption experiments is easier in both experimental procedure and data interpretation. However, pure iron oxide is usually not an appropriate medium for transport experiments due to the very high Fe concentration and thus very high metal adsorbing capacity. In this investigation, we used synthetic goethite-coated sand to mimic natural Fe-coated subsurface materials, while maintaining a relatively simple and controlled chemistry (e.g., one dominant mineral phase, no preadsorbed phosphate, etc.) to facilitate the interpretation of subsequent transport experiments (results not described herein). U(VI) adsorption onto the goethite-coated sand was studied in batch experiments as a function of pH in systems closed to the atmosphere, in the presence and

* Corresponding author phone: (334)844-6291; fax: (334)844-6290; e-mail: barnettm@eng.auburn.edu.

[†] Auburn University.

[‡] University of Alabama.

absence of phosphate. A surface complexation model (SCM) was used to model the data under a range of conditions.

Materials and Methods

Experimental. All chemicals used were certified ACS grade and were obtained from Fisher Scientific (Pittsburgh, PA) unless otherwise mentioned. The acids were TraceMetal grade, and the uranium standards and stock solutions were prepared from plasma grade uranium standard (depleted uranium). The goethite-coated sand was prepared following the methods described by Schwertmann and Cornell (25). In brief, 1000 g of medium sized white quartz (0.210–0.297 mm) from Sigma, 9.9 g unoxidized crystals of $\text{FeCl}_2 \cdot 4\text{H}_2\text{O}$, and 200 mL of 1 M NaHCO_3 were mixed with 1 L of distilled water through which N_2 had been bubbled for 30 min beforehand. During the mixing process, the solution was stirred vigorously and aerated. Oxidation was complete when the color of the suspension changed from green-blue to ochre. The pH during oxidation was self-controlled at about 7 by the NaHCO_3 buffer. After the sand had been coated by goethite, it was rinsed with copious amount of distilled water to remove any electrolyte residues in the solution and on the surface of the sand. The goethite-coated sand was then freeze-dried and stored in clean plastic bags at room temperature for subsequent experiments. The DCB (dithionite–citrate–bicarbonate) extractable Fe (26) of the goethite-coated sand was determined to be $94.3 \pm 2.6 \mu\text{mol}$ of Fe/g of sand, while the AOD (acid ammonium oxalate) extractable Fe (26) of the same goethite-coated sand was determined to be $11.3 \pm 0.4 \mu\text{mol}$ of Fe/g of sand, indicating that the majority of the Fe coating is well-crystallized. The specific surface area of the goethite-coated sand, as measured by BET (Brunauer, Emmett, and Teller) surface analysis (N_2 adsorption) (27), was $1.25 \text{ m}^2/\text{g}$. The specific surface area of the clean (goethite-free) sand measured by the same method was minimal ($<0.01 \text{ m}^2/\text{g}$) as compared to that of goethite-coated sand. Thus, it was assumed that all of the surface area of the goethite-coated sand is due to goethite, and the specific surface area of the goethite coating was calculated to be $149 \text{ m}^2/\text{g}$, based on the measured DCB Fe content and separate determination of surface area of the goethite-coated sand. X-ray diffraction analysis of the Fe coating of a previous batch of Fe-coated sand, prepared using exactly the same method, was performed; the diffraction peaks obtained matched with goethite and showed the broadening expected for the relatively small, high surface area particles (28).

Batch adsorption experiments were conducted at room temperature ($\sim 295 \text{ K}$) in 40-mL polycarbonate centrifuge tubes, each tube yielding one data point. Some of the experiments were performed in duplicate to check the reproducibility of the results. The samples were prepared by adding an appropriate amount of the goethite-coated sand, ionic strength adjuster (NaNO_3), phosphate stock solution (as KH_2PO_4), acidified U(VI) stock solution ($\text{UO}_2(\text{NO}_3)_2$), and distilled deionized water. The tubes were then bubbled with humidified 0.1 M NaOH scrubbed N_2 gas ($P_{\text{CO}_2} = 0 \text{ atm}$) while the pH of the suspensions were adjusted with freshly prepared NaOH and HNO_3 . The volume of the NaOH and HNO_3 used were recorded and found minimal (less than 0.5% of the total solution volume) as compared to the total solution volume, which was 40 mL for all the samples. The change in ionic strength due to pH adjustment was also minimal (less than 4.5% of the total ionic strength). All the samples were prepared rapidly and immediately capped with airtight caps to minimize the exchange of $\text{CO}_2(\text{g})$ with the atmosphere and were gently agitated with a reciprocating shaker table. The experimental conditions are summarized in Table 1. The pH and total U(VI) concentration in batch experiments were within the ranges used by other workers (2, 3, 11, 18, 29) to represent typical pH of groundwater and U(VI)

TABLE 1. Experimental Conditions for Phosphate–U(VI) Adsorption to Goethite-Coated Sand^a

expt ID	solid/solution ratio (g/L)	total Fe(III) (M)	total phosphate (M)	total U(VI) (M)	results shown in
1	3.33	3.15×10^{-4}	0	5×10^{-6}	Figure 2
2	3.33	3.15×10^{-4}	4×10^{-5}	0	Figure 1a
3	3.33	3.15×10^{-4}	2×10^{-4}	0	Figure 1c
4	3.33	3.15×10^{-4}	5×10^{-5}	5×10^{-6}	Figures 1b & 3
5	3.33	3.15×10^{-4}	2×10^{-4}	5×10^{-6}	Figure 1c & 3
6	33.3	3.15×10^{-3}	0	5×10^{-6}	Figure 2
7	33.3	3.15×10^{-3}	10^{-4}	0	Figure 1d
8	33.3	3.15×10^{-3}	10^{-3}	0	Figure 1f
9	33.3	3.15×10^{-3}	10^{-4}	5×10^{-6}	Figures 1d & 4
10	33.3	3.15×10^{-3}	2×10^{-4}	5×10^{-6}	Figures 1e & 4

^a Ionic strength was 0.1 M for all the experiments.

concentration in contaminated groundwater. The phosphate concentration used was higher than phosphate concentration in typical groundwater, which is usually lower than 10^{-5} M (18). This higher phosphate concentration was used for two reasons: (i) phosphorus may be added as a nutrient to contaminated sites in order to promote in situ biological U(VI) reduction to U(IV); (ii) so that phosphate concentration could be high enough so that its effect on U(VI) adsorption can be easily observed and the aqueous phosphate concentration quantified.

After being shaken for 48 h, which had been established as adequate to reach equilibrium by our experiments on adsorption kinetics (data not shown), the samples were removed from the shaker and centrifuged to aid in filtration. The samples were opened, and an aliquot of the supernatant was withdrawn and immediately filtered with a $0.45\text{-}\mu\text{m}$ syringe filter, and the pH of the remaining sand suspension was immediately measured with a pH meter and combination electrode. The filtrate was used to measure the aqueous phosphate and U(VI) concentrations. The phosphate concentration was measured by ion chromatograph (model DX-120, Dionex, Sunnyvale, CA) without further treatment of the filtrate. The U(VI) concentration was analyzed with a KPA (kinetic phosphorescence analyzer) (model KPA-11, Chemchek Instruments, Richland, WA) after acidification of the filtrate to a pH of 1. The uncertainty and detection limit of the U(VI) analysis were $\pm 3\%$ and ca. 10^{-10} M . The centrifugation and filtration were necessary to completely remove from the aqueous phase any tiny amount of solids that may have detached from the goethite-coated sand during the 48 h of equilibration. Even very small amounts of suspended particles in the sample solution may block the ion chromatograph system and interfere with KPA measurement by reflecting and scattering the laser beam. The amount of Fe detached from the goethite-coated sand during the 48 h of shaking was checked for some of the samples and found minimal (less than 0.4% of the total Fe in the goethite coating, except for some extreme cases where pH was below 2, ca. 3% of the total Fe was detached) as compared to the total Fe in the goethite coating. This suggested that the goethite remained completely attached to the sand during equilibration. In addition, the much lower AOD extractable Fe content ($11.3 \mu\text{mol}$ of Fe/g of sand) of the Fe-coated sand as compared to the DCB extractable Fe content ($94.3 \mu\text{mol}$ of Fe/g of sand), which represented total Fe for our goethite-coated sand, further confirmed that the Fe coating should be stable under our experimental conditions. The adsorbed U(VI) concentration was calculated from the difference between the initial and final aqueous U(VI) concentrations. Samples were run with no sand (sand blanks) and with no added U(VI) (U blanks) for controls. There was no loss of U(VI) to the container walls in the sand blanks, and no U(VI) was detected in the U(VI) blanks. Analysis of acid-digested sand residues

TABLE 2. Surface Complexation Reactions Included in Model^a

	eq no.	log K
Acid/Base Properties of Goethite Surface^b		
>FeOH + H ⁺ ↔ >FeOH ₂ ⁺	(1)	7.47
>FeOH ↔ >FeO ⁻ + H ⁺	(2)	-9.51
Phosphate Surface Complexation Reactions^b		
>FeOH + H ₂ PO ₄ ⁻ + H ⁺ ↔ >FePO ₄ H ₂ + H ₂ O	(3)	12.68
>FeOH + H ₂ PO ₄ ⁻ ↔ >FePO ₄ H ⁻ + H ₂ O	(4)	7.93
>FeOH + H ₂ PO ₄ ⁻ ↔ >FePO ₄ ²⁻ + H ⁺ + H ₂ O	(5)	2.16
U(VI) Surface Complexation Reaction^c		
>Fe(OH) ₂ + UO ₂ ²⁺ ↔ (>FeO ₂)UO ₂ ⁰ + 2H ⁺	(6)	-4.66
Ternary Surface Complexation Reaction^c		
>FeOH + UO ₂ ²⁺ + H ₂ PO ₄ ⁻ ↔ >FePO ₄ UO ₂ + H ₂ O + H ⁺	(7)	10.60

^a T = 298 K, I = 0.1 M, constant capacitance model (CCM) with a specific capacitance of 1.28 F/m². ^b From Nilsson et al. (13). ^c Present work.

and acidified container rinseate indicate that these losses of U(VI) to container walls were minimal in the presence of sand for most of the data points. Only at low total Fe concentration (total Fe = 3.15 × 10⁻⁴ M) and high pH (pH > 9.0), the losses were greater than 10%, and those data points were discarded. Although MINTEQA2 4.00 (30) calculation showed some of the initial samples were oversaturated with respect to uranium solids, our kinetics data (not shown) indicated that in our experimental conditions the rate of precipitation was much slower than that of adsorption. So the initial removal of U(VI) from solution was controlled by adsorption and not by precipitation. MINTEQA2 4.00 calculation also verified that the final samples were undersaturated with respect to uranium solids. The MINTEQA2 4.00 calculation and kinetic study confirmed that the removal of U(VI) from solution was due to adsorption.

Modeling. In modeling of our experimental data, we assumed that quartz in the goethite-coated sand was insignificant with respect to adsorption and that surface complexation reactions of phosphate and U(VI) occurred only on the goethite coating. All the aqueous reactions and their stability constants used in our modeling are given in Table S1 in the Supporting Information. The activity coefficients of the charged aqueous species at I = 0.1 M were calculated using the Davies equation (31) to adjust the conditional constants of aqueous reactions at I = 0.1 M. The goodness of fit of the model to the experimental data was quantified by the root-mean-square error (RMSE).

Nilsson et al. (13) modeled the adsorption of phosphate to goethite with three monodentate surface complexes. A constant capacitance model (CCM) was used to account for the electrostatic effects on adsorption. A recent molecular-scale study of the adsorption of phosphate to goethite by atomic force microscope (AFM) confirms that phosphate adsorbs in 1:1 ratio with singly coordinated hydroxyl groups of goethite surface and thus phosphate coordinates monodentately (7). The Nilsson et al. (13) model yielded a satisfactory prediction of our phosphate experimental data, so we used it as a submodel to calculate phosphate adsorption. In our modeling of phosphate adsorption in the absence of U(VI), surface complexation reactions (Table 2, eqs 1–5) and their stability constants from the Nilsson et al. (13) model were adopted without modification. However, the total surface site concentration of our goethite-coated sand was determined by using the computer program FITEQL 4.0 (32) based on our experimental phosphate adsorption data (described below).

To model U(VI) adsorption onto goethite-coated sand in the absence of phosphate, we assumed uranyl ion forms an inner-sphere, mononuclear, bidentate surface complex (29),

which has been successful in predicting U(VI) adsorption to both synthetic pure iron oxyhydroxides and heterogeneous natural subsurface materials (2, 24, 29). The U(VI) surface complexation reaction is presented in Table 2. The CCM, which is consistent with the model used to compute phosphate adsorption, was used to account for electrostatic effects. The total surface site of the goethite-coated sand had been determined before from phosphate adsorption data. The surface complexation reactions included in our modeling of U(VI) adsorption in the absence of phosphate are listed in Table 2 (eqs 1, 2, and 6). The stability constant of U(VI) surface complexation reaction (eq 6 in Table 2) was determined by using FITEQL 4.0 based on our experimental U(VI) adsorption data in the absence of phosphate.

To model U(VI) adsorption in the presence of phosphate, besides all the surface complexation reactions used in modeling phosphate and U(VI) adsorption, ternary surface complexation reaction (eq 7 in Table 2) are also required. All the constants of aqueous reactions, acid/base properties of goethite, and phosphate surface complexation reactions were obtained from previous literature (2, 13, 33). The total surface site concentration of the goethite-coated sand and the stability constant of U(VI) surface complexation reaction (eq 6 in Table 2) had been determined earlier in the present work. The only unknown was the stability constant of the ternary surface complexation reaction. This value was determined by using FITEQL 4.0 based on our experimental U(VI) adsorption data in the presence of phosphate.

Results and Discussion

Phosphate Adsorption. The adsorption of phosphate onto the surface of goethite-coated sand is shown in Figure 1a–f. Phosphate strongly adsorbed to goethite, and the extent of adsorption decreased with increasing pH. The Nilsson et al. model (13) was adopted to calculate phosphate adsorption in our modeling (solid lines, Figure 1). All the reactions with their constants from the Nilsson et al. model (13) were used in our calculation without modification. However, the total surface site density in our calculation was obtained with FITEQL 4.0. Using the data from experiment 3, the fitted total surface site concentration was 2.23 × 10⁻⁵ mol/L. Assuming all of the surface area is due to goethite and not to quartz, this value corresponds to a surface site density of 3.23 sites/nm². The surface site density obtained is in the range of reported site density of goethite (2.3–10 sites/nm²) (11), and this value was used in all our remaining calculations.

U(VI) Adsorption. The adsorption of U(VI) onto the surface of goethite in the absence of phosphate is shown in Figure 2. The extent of U(VI) adsorbed was strongly dependent on solution pH. Below pH 4.0, at total Fe concentration of 3.15 × 10⁻⁴ M, almost all U(VI) remained in the aqueous phase. The percentage of U(VI) adsorbed increased sharply between pH 4 and pH 6, and more than 99% of the U(VI) was adsorbed above pH 6. The pH edge shifted to the left with an increase in total Fe concentration from 3.15 × 10⁻⁴ to 3.15 × 10⁻³ M, indicating more U(VI) adsorption at the same pH due to a higher concentration of available surface sites. U(VI) adsorption in the absence of phosphate was modeled using the surface complexation reactions and stability constants in Table 2 and aqueous reactions in Table S1 in the Supporting Information. The total surface site density was fixed at 3.23 sites/nm², the same as that used in simulations of phosphate adsorption. The stability constant for UO₂²⁺ adsorption onto goethite surface was determined to be log K = -4.66 using FITEQL 4.0, based on the experimental data from experiment 6 (total Fe concentration = 3.15 × 10⁻³ M, Figure 2). The model gave an excellent fit of the experimental data (Figure 2, solid line). The same model was used to predict U(VI) adsorption at total Fe concentration of 3.15 × 10⁻⁴ M (Figure 2 dashed line). The model correctly predicted the right-shift

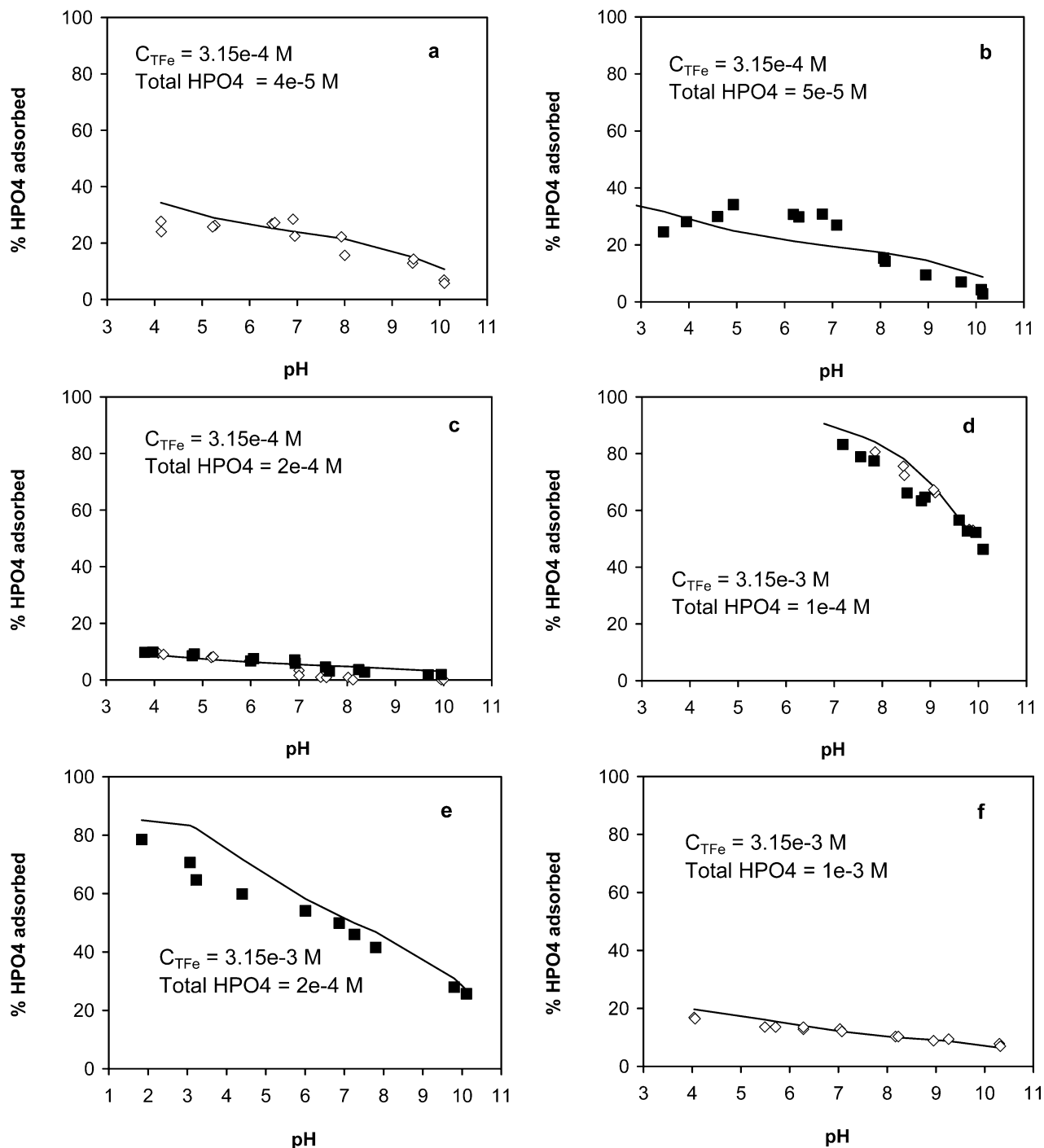


FIGURE 1. Adsorption of phosphate onto goethite-coated sand in the absence (\diamond) and presence (\blacksquare) of 5×10^{-6} M U(VI). The solid lines are prediction by the Nilsson et al. model, assuming no U(VI) present. $I = 0.1$ M, $T = 295$ K. The RMSE between the model prediction and the experimental data is as follows: (a) 0.044; (b) 0.082; (c) 0.029 (no U(VI)), 0.012 (U(VI) = 5×10^{-6} M); (d) 0.029 (no U(VI)), 0.063 (U(VI) = 5×10^{-6} M); (e) 0.095; (f) 0.015.

of the pH edge, and the predicted values were close to experimental results, although adsorption was generally overestimated. U(VI) adsorption to pure goethite or goethite-coated sand in the absence of phosphate has been modeled by other workers (11, 34). The stability constant of U(VI) surface complex with goethite in those models cannot be directly compared to that in our model due to the difference in the modeling approaches. However, calculated U(VI) adsorption by the Gabriel et al. model (34) agreed well with our experimental data, indicating that our U(VI) adsorption data in the absence of phosphate was consistent with those previous results.

U(VI)–Phosphate Ternary Systems. The adsorption of phosphate onto the surface of goethite-coated sand in the presence of U(VI) is shown in Figure 1b–e. The presence of U(VI) did not have an appreciable effect on phosphate adsorption when phosphate concentration was much higher (total phosphate/total U(VI) > 20) than that of U(VI) (Figure 1c,d). Yet, when the phosphate concentration was not much higher than the U(VI) concentration, in the pH range of 5.0–7.0, an increase in phosphate adsorption was observed (Figure 1b) relative to that predicted by the Nilsson et al. model. In this pH range, the adsorption of U(VI) was almost complete (data not shown). Payne et al. (18) reported similar results

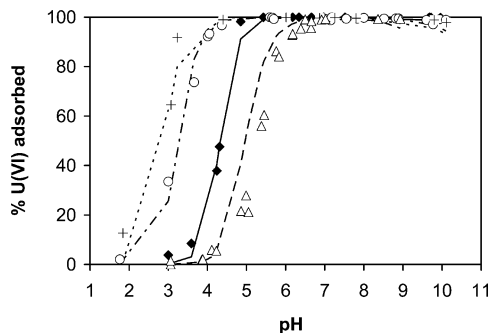


FIGURE 2. Adsorption of 5×10^{-6} M U(VI) onto goethite-coated sand at total Fe concentration of 3.15×10^{-4} in the absence of phosphate (Δ) and at total Fe concentration of 3.15×10^{-3} M in the absence of phosphate (\blacklozenge) and at phosphate concentrations of 10^{-4} M (\circ) and 2×10^{-4} M ($+$). $I = 0.1$ M, $T = 295$ K. The symbols are experimental data, and the lines are model prediction. In the absence of phosphate, the RMSE of predictions is 0.028 and 0.135 at total Fe concentration of 3.15×10^{-3} and 3.15×10^{-4} M, respectively. In the presence of phosphate, the RMSE is 0.032 and 0.056 for total phosphate concentration of 10^{-4} and 2×10^{-4} M, respectively.

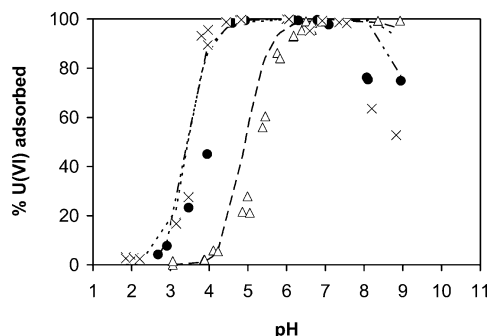


FIGURE 3. Adsorption of 5×10^{-6} M U(VI) onto goethite-coated sand at total Fe concentration of 3.15×10^{-4} M in the absence of phosphate (Δ) and at phosphate concentrations of 5×10^{-5} M (\bullet) and 2×10^{-4} M (\times). $I = 0.1$ M, $T = 295$ K. The symbols are experimental data, and the lines are model prediction. The RMSE of predictions is 0.135, 0.172, and 0.140 for total phosphate concentration of 0, 5×10^{-5} and 2×10^{-4} M, respectively.

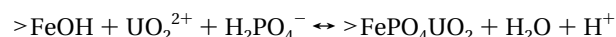
in their study of the effects of phosphate on U(VI) adsorption onto ferrihydrite. A plausible explanation for the increased adsorption of phosphate is the formation of a ternary surface complex containing both U(VI) and phosphate, which increases the adsorption of both U(VI) and phosphate (see further discussion below).

The effect of phosphate on U(VI) adsorption at total Fe concentrations of 3.15×10^{-3} and 3.15×10^{-4} M are shown in Figures 2 and 3. In the low pH range, the addition of phosphate greatly increased U(VI) adsorption. Higher phosphate concentration generally caused a greater effect (Figure 2), although the extent of the effect was sometimes negligible (Figure 3). Payne et al. (18) reported increased U(VI) adsorption onto ferrihydrite in the presence of 10^{-4} M phosphate at pH 3.0–6.0, where phosphate was strongly adsorbed to the oxide surface. Bostick et al. (19) also showed that when adding U(VI) to natural subsurface samples, strong adsorbed inner-sphere U(VI) phosphate complexes formed at low pH, presumably from preexisting natural phosphate adsorbed to iron(III) oxides. Our experimental data indicated strong phosphate adsorption for those data points where U(VI) adsorption was enhanced by phosphate (Figures 1 and 2). Together these results suggest that a ternary surface complex is formed under these conditions and should be included in the modeling in order to correctly predict U(VI) adsorption in the presence of phosphate. The structure of

the ternary surface complex is not known at this time due to the absence of spectroscopic data. Recently, formation of inner-sphere, bidentate surface complex of U(VI) on hydroxyapatite has been verified by spectroscopic study (35). A ternary complex of dissolved phosphate with adsorbed U(VI), in the form of $(>CaO_2)UO_2PO_4$, and/or U(VI) bonding to phosphate surface sites, in the form of $(>PO_2)UO_2$, were both possible structures for U(VI) surface complexes formed on hydroxyapatite. It is possible that the U(VI) surface complex formed on goethite in the presence of phosphate may have similar structure as those on hydroxyapatite.

In the high pH range, at total Fe concentration of 3.15×10^{-3} M, the presence of 10^{-4} or 2×10^{-4} M phosphate did not cause any appreciable decrease in U(VI) adsorption (Figure 2), which seems to contradict Payne et al.'s results (18). However, in the Payne et al. experiments, the samples were in equilibrium with atmospheric CO_2 , and at high pH, the carbonate concentration of the solution was very high, in which case the decrease in U(VI) adsorption may have been caused by the formation of highly soluble U(VI)–carbonate species (e.g., $UO_2(CO_3)_3^{4-}$) (2, 18, 29) rather than by U(VI)–phosphate species. At a total Fe concentration of 3.15×10^{-4} M, the presence of 5×10^{-5} or 2×10^{-4} M phosphate did lead to a decrease in U(VI) adsorption at pH > 8.0 , and a higher total phosphate concentration resulted in a greater decrease in U(VI) adsorption (Figure 3). Since carbonate was excluded in our experiments (as evidenced by near 100% adsorption of U(VI) at high pH shown in Figures 2), the decrease in U(VI) adsorption was not due to the formation of soluble U(VI)–carbonate complexes. Rather, formation of soluble U(VI) complexes such as $UO_2PO_4^-$ might have caused the observed decrease in U(VI) adsorption.

To model U(VI) adsorption onto goethite in the presence of phosphate, a ternary surface complex between U(VI) and phosphate was required. In the absence of spectroscopic data that provides detailed structural information on the surface complex formed, determination of surface stoichiometries is usually made from trials for data simulation performance. Ternary surface complexes of type A, in the form of $>FeOML$, where M is metal ion and L is a generic ligand, as discussed by Schindler (36), was used in our preliminary fitting. However, this type of species were unable to account for the decrease in U(VI) adsorption at high pH values in the U(VI)–phosphate ternary systems. Thus, a type B complex (36), in the form of $>FeLM$, was considered as an alternative surface complex between uranium and phosphate. The stoichiometry of the proposed ternary species is



In our modeling of U(VI) adsorption onto goethite in the presence of phosphate, all the reactions and stability constants in Tables 2 and Table S1 in the Supporting Information were included. The total surface site of the goethite-coated sand and stability constant of U(VI) surface complexation reaction (eq 6 in Table 2) had been determined earlier in the present work. The only unknown was the stability constant of the ternary surface complexation reaction, and this value was determined by using FITEQL 4.0 based on data from experiment 9 (Figure 2). The stability constant thus obtained was $\log K = 10.60$. Payne et al. (18) postulated the same ternary surface complex to fit their U(VI) adsorption data in the ferrihydrite/uranium/phosphate system. However, no modeling results or the value of the stability constant for the ternary surface complex was published. Qualitatively, our proposed stability constant for the ternary surface complex was in agreement with the Payne et al. experimental data. A subsequent paper will present an evaluation of the ability of our model to predict the Payne et al. data.

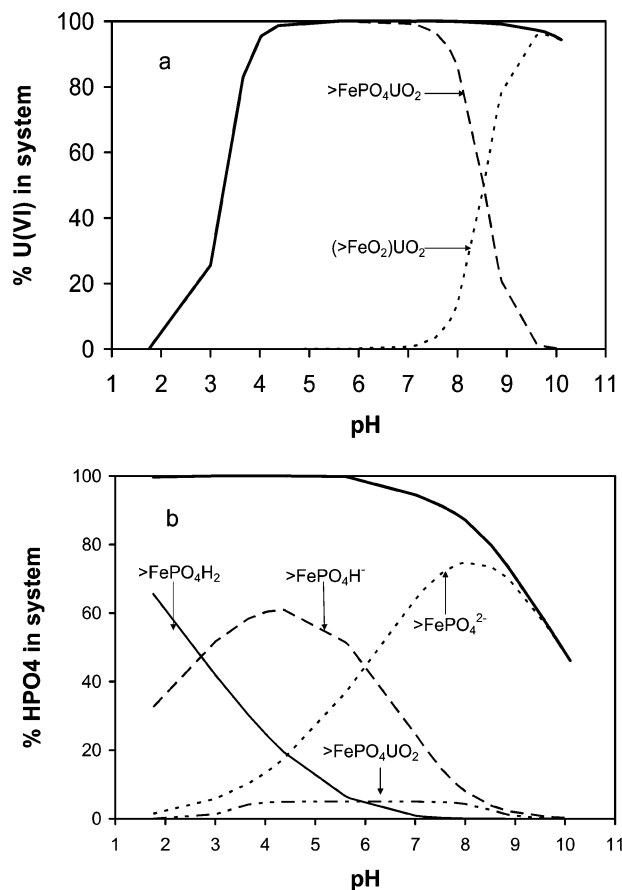


FIGURE 4. Model calculation of (a) U(VI) and (b) phosphate surface speciation. Total Fe concentration was 3.15×10^{-3} M, total U(VI) concentration was 5×10^{-6} M, and total phosphate concentration was 10^{-4} M. $I = 0.1$ M, $T = 295$ K. The thick full line represents total adsorbed U(VI) or phosphate predicted by the model. The thin full line and dash lines represent U(VI) or phosphate surface complexes calculated by the model.

The adsorption of U(VI) at different total phosphate concentrations and total Fe concentrations predicted by the model are shown in Figures 2 and 3. At a total Fe concentration of 3.15×10^{-3} M, the shape of the pH edge predicted by the model is in agreement with the experimental results for the whole pH range (Figure 2). The model predicts the shift of the pH edge to the left with increasing phosphate concentration. At a total Fe concentration of 3.15×10^{-4} M, the model correctly predicted the U(VI) pH edge for both total phosphate concentrations in the range of $\text{pH} < 7.0$ (although adsorption is overestimated for some data points with pH between 3.0 and 4.0), and indicated that the U(VI) pH edges for the two phosphate concentrations should overlap, which agreed with our experimental data (Figure 3). At $\text{pH} > 7.0$, the model predicted some decrease in U(VI) adsorption, which agreed with experimental data. However, the model failed to consistently generate the shape of the experimental adsorption edge at $\text{pH} > 7$. For both phosphate concentrations, U(VI) adsorption was overpredicted by the model. If our model is correct, the decrease in U(VI) adsorption in the presence of phosphate at high pH was mainly due to the formation of soluble complexes, such as UO_2PO_4^- . As previously discussed, the adsorption of phosphate onto goethite is predicted accurately in our model. In addition, the formation constant of $\text{UO}_2(\text{OH})_3^-$ is well-established. Thus, we may provisionally attribute the disagreement between our model predictions and experimental data at high pH in the presence of phosphate to uncertainty in the current database for aqueous U(VI)–phosphate species

in this pH range. In the pH range of 6–9, the stability constants of the aqueous U(VI)–phosphate complexes have an inherent uncertainty due to the low free-uranyl concentration under the experimental conditions in which these constants are determined (14). Moreover, the nature of the aqueous U(VI)–phosphate complexes formed in alkaline solutions is uncertain. Both aqueous $\text{UO}_2(\text{PO}_4)_{n-3n}^{2-3n}$ ($n > 1$) and mixed hydroxide–phosphate complexes might be expected (14) but have not been included in the current database. On the basis of our results, it seems likely that the stability constants of soluble uranium–phosphate complexes in the current database might be underestimated, and the existence of aqueous $\text{UO}_2(\text{PO}_4)_{n-3n}^{2-3n}$ ($n > 1$) and mixed hydroxide–phosphate complexes is possible.

To visualize the proposed reactions, the model calculated speciation of surface complexes of U(VI) and phosphate for experiment 9 are shown in Figure 4. In the presence of phosphate the increased U(VI) adsorption in the low pH range was due to the formation of ternary surface complex (Figure 4a). In the absence of phosphate, from pH 3 to pH 10, the binary U(VI) surface complex was responsible for U(VI) adsorption (Figure 2). While in the presence of phosphate, the ternary surface complex was responsible for U(VI) adsorption from pH 2 to pH 6, and it was the dominant U(VI) surface complex at $\text{pH} < 8$. In the presence of phosphate, only at $\text{pH} > 6$, the binary U(VI) surface complex began to form, and at $\text{pH} > 8.5$, it became the dominant U(VI) surface complex. The addition of phosphate to the system changed the mechanisms of U(VI) adsorption. From Figure 4b, it is seen that the dominant phosphate surface complex changed from $>\text{FePO}_4\text{H}_2$, to $>\text{FePO}_4\text{H}^-$ and to $>\text{FePO}_4^{2-}$ as the solution pH increased. The concentration of the ternary surface complex was always much lower than other phosphate surface complexes due to the low total U(VI) concentration in the system. The ternary surface complex reached its highest concentration in the pH range of 4–7, where almost 100% of U(VI) formed the ternary surface complex.

Environmental Implications

Phosphate will decrease the mobility of U(VI) in the presence of iron oxyhydroxides such as goethite through the formation of ternary surface complexes at acidic pH . The adsorption of both U(VI) and phosphate will be increased by the formation of this ternary surface complex, which is likely to be the dominant surface species at low pH . At higher pH , the presence of phosphate may decrease U(VI) adsorption at low total Fe concentrations, through the formation of soluble U(VI)–phosphate species. Quantitatively the surface complexation model developed provided reasonable predictions of U(VI) and phosphate adsorption under a range of conditions such as total Fe concentration, total phosphate concentration, and pH . However, the stoichiometry and structure of our proposed ternary U(VI)–phosphate complex formed on the surface of goethite needs to be confirmed by spectroscopic study. At low total Fe concentration and alkaline pH , the disparity between model prediction and experimental data is attributed to the formation of possible aqueous $\text{UO}_2(\text{PO}_4)_{n-3n}^{2-3n}$ ($n > 1$) and mixed hydroxide–phosphate complexes that are not included in the current database as well as the underestimation of formation constant(s) for aqueous U(VI)–phosphate species in the current database. Experimental study is necessary to obtain more accurate information on the types of complex species formed in alkaline solution and their stability constants in order to accurately predict U(VI) mobility in the high pH range.

Acknowledgments

The authors acknowledge the comments of four anonymous reviewers that greatly improved the paper. This research was

supported by Grant DE-FG07-ER6321 from the U.S. Department of Energy Environmental Management and Science Program.

Supporting Information Available

One table showing the aqueous reactions included in the model. This material is available free of charge via the Internet at <http://pubs.acs.org>.

Literature Cited

- (1) Duff, M. C.; Amrhein, C. Uranium(VI) adsorption on goethite and soil in carbonate solutions. *Soil Sci. Soc. Am. J.* **1996**, *60*, 1393–1400.
- (2) Barnett, M. O.; Jardine, P. M.; Brooks, S. C. U(VI) adsorption to heterogeneous subsurface media: application of a surface complexation model. *Environ. Sci. Technol.* **2002**, *36*, 937–942.
- (3) Barnett, M. O.; Jardine, P. M.; Brooks, S. C.; Selim, H. M. Adsorption and transport of uranium(VI) in subsurface media. *Soil Sci. Soc. Am. J.* **2000**, *64*, 908–917.
- (4) Casas, I.; Casabona, D.; Duro, L.; Depablo, J. The influence of hematite on the sorption of uranium(VI) onto granite filling fractures. *Chem. Geol.* **1994**, *113*, 319–326.
- (5) Ticknor, K. V. Uranium sorption on geological materials. *Radiochim. Acta* **1994**, *64*, 229–236.
- (6) Cornell, R. M.; Schwertmann, U. *The Iron Oxides*; VCH: New York, 1996.
- (7) Dideriksen, K.; Stipp, S. L. S. The adsorption of glyphosate and phosphate to goethite: a molecular-scale atomic force microscopy study. *Geochim. Cosmochim. Acta* **2003**, *67*, 3313–3327.
- (8) Gao, Y.; Mucci, A. Acid base reactions, phosphate and arsenate complexation, and their competitive adsorption at the surface of goethite in 0.7 M NaCl solution. *Geochim. Cosmochim. Acta* **2001**, *65*, 2361–2378.
- (9) Villalobos, M.; Leckie, J. O. Carbonate adsorption on goethite under closed and open CO₂ conditions. *Geochim. Cosmochim. Acta* **2000**, *64*, 3787–3802.
- (10) Villalobos, M.; Leckie, J. O. Surface complexation modeling and FTIR study of carbonate adsorption to goethite. *J. Colloid Interface Sci.* **2001**, *235*, 15–32.
- (11) Villalobos, M.; Trotz, M. A.; Leckie, J. O. Surface complexation modeling of carbonate effects on the adsorption of Cr(VI), Pb(II), and U(VI) on goethite. *Environ. Sci. Technol.* **2001**, *35*, 3849–3856.
- (12) Geelhood, J. S.; Hiemstra, T.; Riemsdijk, W. H. V. Phosphate and sulfate adsorption on goethite: single anion and competitive adsorption. *Geochim. Cosmochim. Acta* **1997**, *61*, 2389–2396.
- (13) Nilsson, N.; Lovgren, L.; Sjoberg, S. Phosphate complexation at the surface of goethite. *Chem. Speciation Bioavailability* **1992**, *4*, 121–130.
- (14) Sandino, A.; Bruno, J. The solubility of (UO₂)₃(PO₄)₂·4H₂O and the formation of U(VI) phosphate complexes: their influence in uranium speciation in natural waters. *Geochim. Cosmochim. Acta* **1992**, *56*, 4135–4145.
- (15) Abdelouas, A.; Lu, Y. M.; Lutze, W.; Nuttall, H. E. Reduction of U(VI) to U(IV) by indigenous bacteria in contaminated ground water. *J. Contam. Hydrol.* **1998**, *35*, 217–233.
- (16) Barton, L. L.; Choudhury, K.; Thomson, B. M.; Steenhoudt, K.; Groffman, A. R. Bacterial reduction of soluble uranium: the first step of in situ immobilization of uranium. *Radioact. Waste Manage. Environ. Restor.* **1996**, *20*, 141–151.
- (17) Lovley, D. R.; Phillips, E. J. P. Bioremediation of uranium contamination with enzymatic uranium reduction. *Environ. Sci. Technol.* **1992**, *26*, 2228–2234.
- (18) Payne, T. E.; Davis, J. A.; Waite, T. D. Uranium adsorption on ferrihydrite—effects of phosphate and humic acid. *Radiochim. Acta* **1996**, *74*, 239–243.
- (19) Bostick, B. C.; Fendorf, S.; Barnett, M. O.; Jardine, P. M.; Brooks, S. C. Uranyl surface complexes formed on subsurface media from DOE facilities. *Soil Sci. Soc. Am. J.* **2002**, *66*, 99–108.
- (20) Arey, J. S.; Seaman, J. C.; Bertsch, P. M. Immobilization of uranium in contaminated sediments by hydroxyapatite addition. *Environ. Sci. Technol.* **1999**, *33*, 337–342.
- (21) Jerden, J. L., Jr.; Sinha, A. K. Phosphate based immobilization of uranium in an oxidizing bedrock aquifer. *Appl. Geochem.* **2003**, *18*, 823–843.
- (22) Sato, T.; Murakami, T.; Yanase, N.; Isobe, H.; Payne, T. E.; Airey, P. L. Iron nodules scavenging uranium from groundwater. *Environ. Sci. Technol.* **1997**, *31*, 2854–2858.
- (23) Coston, L. A.; Fuller, C. C.; Davies, J. A. Pb²⁺ and Zn²⁺ adsorption by a natural aluminum- and iron-bearing surface coating on an aquifer sand. *Geochim. Cosmochim. Acta* **1995**, *59*, 3535–3547.
- (24) Logue, B. A.; Smith, R. W.; Westall, J. C. U(VI) adsorption on natural iron-coated sands: comparison of approaches for modeling adsorption on heterogeneous environmental materials. *Appl. Geochem.* (in press).
- (25) Schwertmann, U.; Cornell, R. M. *Iron Oxides in the Laboratory*; VCH: New York, 1991.
- (26) Jackson, M. L.; Lim, C. H.; Zelazny, L. W. In *Methods of Soil Analysis*, Part 1; Klute, A., Ed.; Soil Science Society of America: Madison, WI, 1986; pp 113–119.
- (27) Brunauer, S.; Emmeet, P. H.; Teller, E. Adsorption of gases in multimolecular layers. *Am. Chem. Soc. J.* **1938**, *60*, 309–319.
- (28) Roden, E. E.; Urrutia, M. M.; Mann, C. J. Bacterial reductive dissolution of crystalline Fe(III) oxide in continuous-flow column reactors. *Appl. Environ. Microbiol.* **2000**, *66*, 1062–1065.
- (29) Waite, T. D.; Davis, J. A.; Payne, T. E.; Waychunas, G. A.; Xu, N. Uranium(VI) adsorption to ferrihydrite: application of a surface complexation model. *Geochim. Cosmochim. Acta* **1994**, *58*, 5465–5478.
- (30) Allison, J. D.; Brown, D. S.; Novo-Gradac, K. J. *MINTEQA2/PRODEFA2, A Geochemical Assessment Model for Environmental Systems: Version 3.0 User's Manual*; U.S. EPA: Athens, GA, 1991.
- (31) Davies, C. W. The extent of dissociation of salts in water. VII. An equation for the mean ionic activity coefficient of an electrolyte in water, and a revision of the dissociation constant of some sulphates. *J. Chem. Soc. Part 2* **1938**, 2093–2098.
- (32) Herbelin, A. L.; Westall, J. C. *FITEQL: A Computer Program for Chemical Equilibrium Constants from Experimental Data. Report 99-01, Version 4.0*; Department of Chemistry, Oregon State University: Corvallis, OR, 1999.
- (33) Grenthe, I.; Fuger, J.; Konings, R. J. M.; Lemire, R. J.; Mueller, A. B.; Nguyen-Trung, C.; Wanner, H. *Chemical Thermodynamics of Uranium*; North-Holland: New York, 1992.
- (34) Gabriel, U.; Gaudet, J.-P.; Spadini, L.; Charlet, L. Reactive transport of uranyl in a goethite column: an experimental and modelling study. *Chem. Geol.* **1998**, *151*, 107–128.
- (35) Fuller, C. C.; Bargar, J. R.; Davis, J. A.; Piana, M. J. Mechanisms of uranium interactions with hydroxyapatite: implications for groundwater remediation. *Environ. Sci. Technol.* **2002**, *36*, 158–165.
- (36) Schindler, P. W. In *Mineral-Water Interface Geochemistry*; Hochella, M. F., Jr., White, A. F., Eds.; Mineralogical Society of America: Washington, DC, 1990.

Received for review March 19, 2004. Revised manuscript received August 18, 2004. Accepted August 31, 2004.

ES0403880

Supporting Information

Journal: *Environ. Sci. Technol.*

Manuscript Title: The Effects of Phosphate on Uranium(VI) Adsorption to Goethite-coated Sand

Tao Cheng[†], Mark O. Barnett^{*†}, Eric E. Roden[‡], and Jinling Zhuang[†]

Department of Civil Engineering, 238 Harbert Engineering Center, Auburn University, Auburn, AL 36849, and Department of Biological Sciences, A122 Bevill Bldg 7th Ave, University of Alabama, Tuscaloosa, AL 35487-0206

* Corresponding author phone: (334) 844-6291; fax: (334) 844-6290; e-mail: barnettm@eng.auburn.edu

[†] Auburn University.

[‡] University of Alabama.

Table S1. Aqueous Reactions Included in Model (T = 298 K)

		log K (I = 0.1 M)	log K (I = 0)
Water Hydrolysis Reaction			
$\text{H}_2\text{O} \leftrightarrow \text{H}^+ + \text{OH}^-$	(1)	-13.78	-13.99
Phosphate Acid-base Reactions ^a			
$\text{H}^+ + \text{H}_2\text{PO}_4^- \leftrightarrow \text{H}_3\text{PO}_4$	(2)	1.90	1.68
$\text{H}_2\text{PO}_4^- \leftrightarrow \text{HPO}_4^{2-} + \text{H}^+$	(3)	-6.71	-6.27
$\text{H}_2\text{PO}_4^- \leftrightarrow \text{PO}_4^{3-} + 2\text{H}^+$	(4)	-18.45	-17.35
U(VI) Complexation Reactions with Water ^b			
$\text{UO}_2^{2+} + \text{H}_2\text{O} \leftrightarrow \text{UO}_2\text{OH}^+ + \text{H}^+$	(5)	-5.41	-5.20
$\text{UO}_2^{2+} + 2\text{H}_2\text{O} \leftrightarrow \text{UO}_2(\text{OH})_2^0 + 2\text{H}^+$	(6)	-12.23 ^c	-12.02 ^c
$\text{UO}_2^{2+} + 3\text{H}_2\text{O} \leftrightarrow \text{UO}_2(\text{OH})_3^- + 3\text{H}^+$	(7)	-20.00	-19.20
$\text{UO}_2^{2+} + 4\text{H}_2\text{O} \leftrightarrow \text{UO}_2(\text{OH})_4^{2-} + 4\text{H}^+$	(8)	-32.57	-33.00
$3\text{UO}_2^{2+} + 5\text{H}_2\text{O} \leftrightarrow (\text{UO}_2)_3(\text{OH})_5^+ + 5\text{H}^+$	(9)	-16.22	-15.55
$4\text{UO}_2^{2+} + 7\text{H}_2\text{O} \leftrightarrow (\text{UO}_2)_4(\text{OH})_7^+ + 7\text{H}^+$	(10)	-22.62	-21.90
$2\text{UO}_2^{2+} + 2\text{H}_2\text{O} \leftrightarrow (\text{UO}_2)_2(\text{OH})_2^{2+} + 2\text{H}^+$	(11)	-5.79	-5.62
$3\text{UO}_2^{2+} + 7\text{H}_2\text{O} \leftrightarrow (\text{UO}_2)_3(\text{OH})_7^- + 7\text{H}^+$	(12)	-31.29	-31.00
$2\text{UO}_2^{2+} + \text{H}_2\text{O} \leftrightarrow (\text{UO}_2)_2\text{OH}^{3+} + \text{H}^+$	(13)	-2.44	-2.70
$3\text{UO}_2^{2+} + 4\text{H}_2\text{O} \leftrightarrow (\text{UO}_2)_3(\text{OH})_4^{2+} + 4\text{H}^+$	(14)	-12.25	-11.90
U(VI) Complexation Reactions with Phosphate ^b			
$\text{UO}_2^{2+} + \text{PO}_4^{3-} \leftrightarrow \text{UO}_2\text{PO}_4^-$	(15)	11.89	13.23
$\text{UO}_2^{2+} + \text{HPO}_4^{2-} \leftrightarrow \text{UO}_2\text{HPO}_4^0$	(16)	6.35	7.24
$\text{UO}_2^{2+} + \text{H}_3\text{PO}_4(\text{aq}) \leftrightarrow \text{UO}_2\text{H}_2\text{PO}_4^+ + \text{H}^+$	(17)	0.90	1.12
$\text{UO}_2^{2+} + \text{H}_3\text{PO}_4(\text{aq}) \leftrightarrow \text{UO}_2\text{H}_3\text{PO}_4^{2+}$	(18)	0.76	0.76
$\text{UO}_2^{2+} + 2\text{H}_3\text{PO}_4(\text{aq}) \leftrightarrow \text{UO}_2(\text{H}_2\text{PO}_4)_2^0 + 2\text{H}^+$	(19)	0.41	0.64
$\text{UO}_2^{2+} + 2\text{H}_3\text{PO}_4(\text{aq}) \leftrightarrow \text{UO}_2(\text{H}_2\text{PO}_4)(\text{H}_3\text{PO}_4)^+ + \text{H}^+$	(20)	1.42	1.65
^a from Nilsson <i>et al.</i> (13)			
^b from Grenthe <i>et al.</i> (33) unless otherwise noted, corrected for ionic strength			
^c from Barnett <i>et al.</i> (2)			